Seminar Presentation

3D Imaging, Analysis, and Guidance for Robotic-Assisted Ankle Fracture / Dislocation Surgery

Asef Islam

Group 10

Mentors:

Dr. Jefferey Siewerdsen

Dr. Wojtek Zbijewski

JOHNS HOPKINS
WHITING SCHOOL of ENGINEERING

I-STAR

The I-STAR Lab
Imaging for Surgery, Therapy, and Radiology

Project Goal

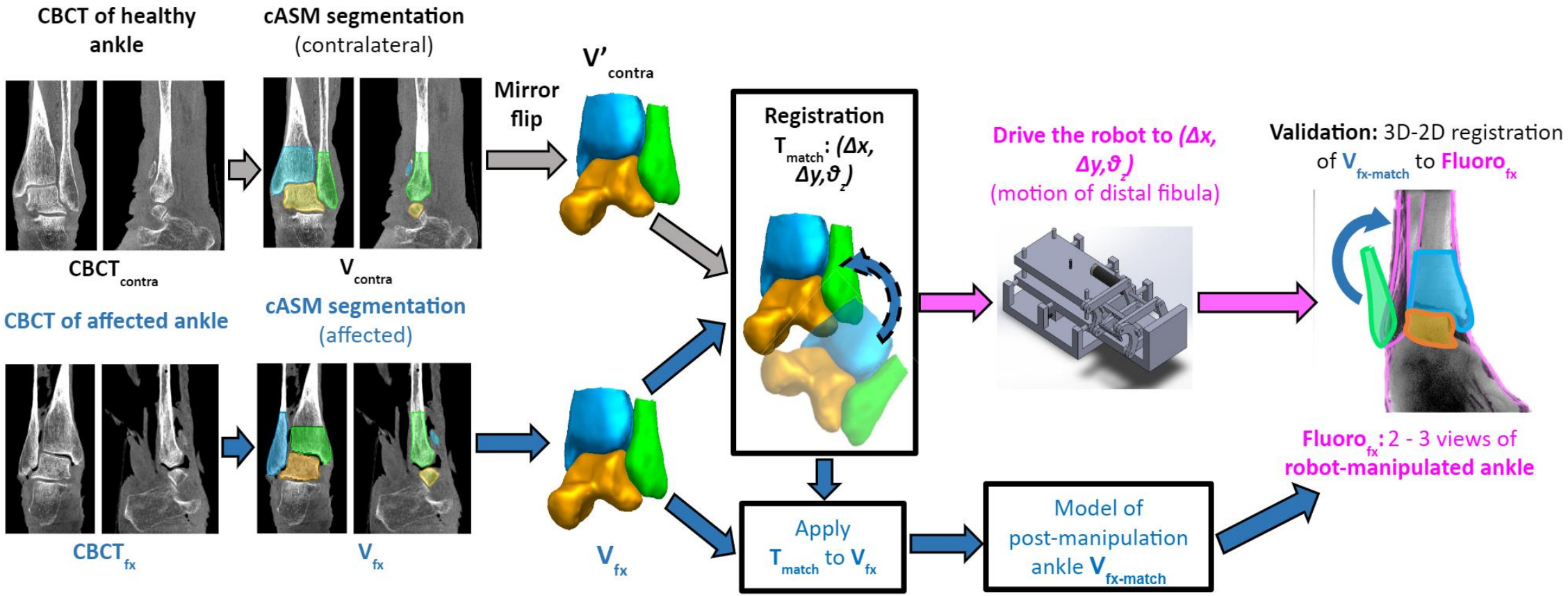

Figure by Wojtek Zbijewski

- Key Step is Automatic Segmentation

Papers Selected

[1] Görres, J., Brehler, M., Franke, J. *et al.* Articular surface segmentation using active shape models for intraoperative implant assessment. *Int J CARS* **11,** 1661–1672 (2016).

[2] Brehler M, Islam A, Vogelsang L, et al. Coupled Active Shape Models for Automated Segmentation and Landmark Localization in High-Resolution CT of the Foot and Ankle. *Proc SPIE Int Soc Opt Eng*. 2019.

Paper 1: Purpose and Significance

- Improve segmentations of ankle bones for improved surgical accuracy of implant placement in articular regions
- Introduce ASM framework for automatic segmentation
- Assess segmentation error and accuracy in intra-articular implants

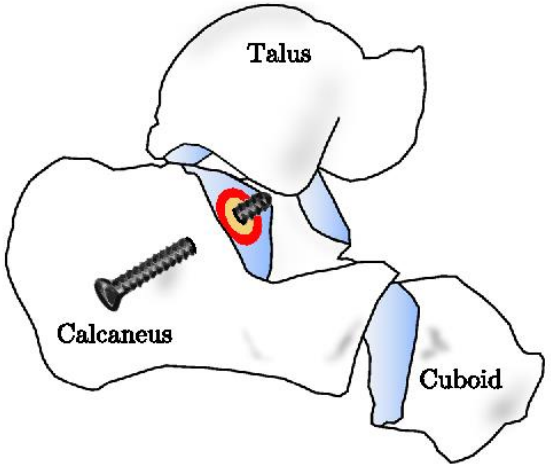

ASM Construction

- Trained on a set of segmentations of the bone with landmark points that are represented in 3-dimensional space
- Used to model morphological variance and create deformable model

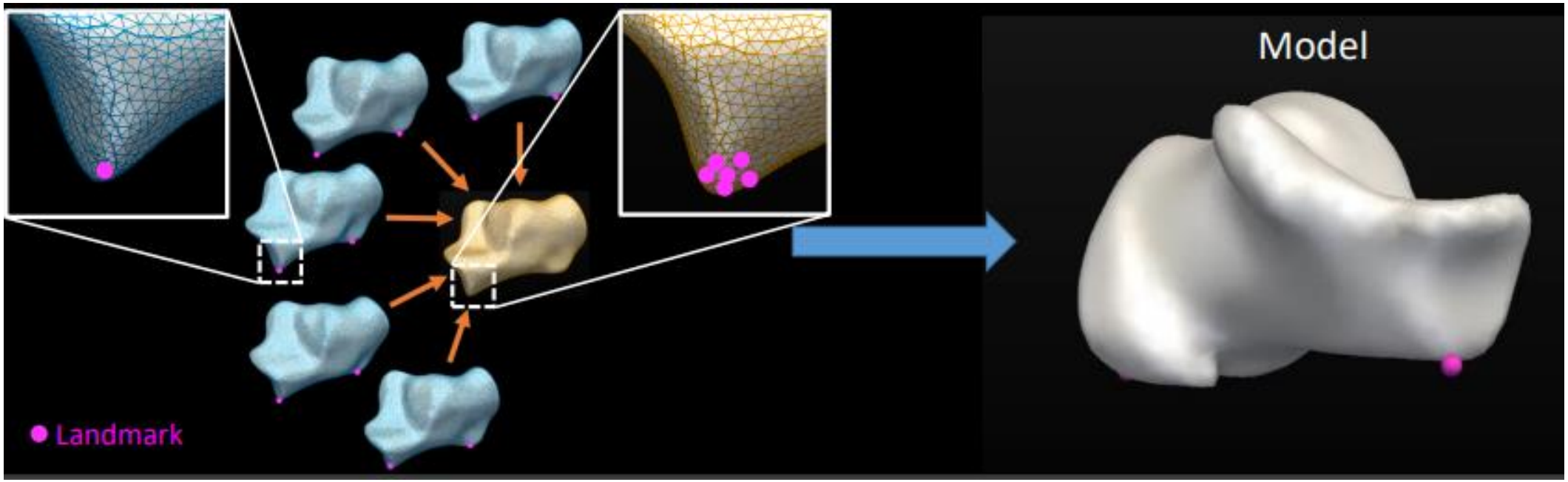

ASM Construction

- Each training set segmentation represented as a point in 3n space (3 * n landmark points)
- PCA used to project 3D landmark points into t principal modes of variance, reducing total dimensionality from 3n to t
- P is projection matrix, b is vector of magnitudes of variation in each mode to represent shape
- Any example x can be represented as mean shape, $\bar{x}$, plus variation (P * b)

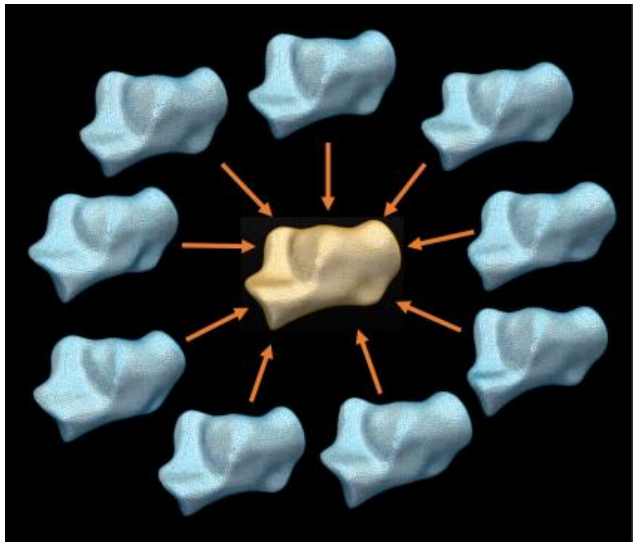

n landmark points
t principal components

$$\mathbf{x} \approx \bar{\mathbf{x}} + \mathbf{Pb}$$

x and $\bar{x}$: 3n x 1
P: 3n x t
b: t x 1

ASM Construction

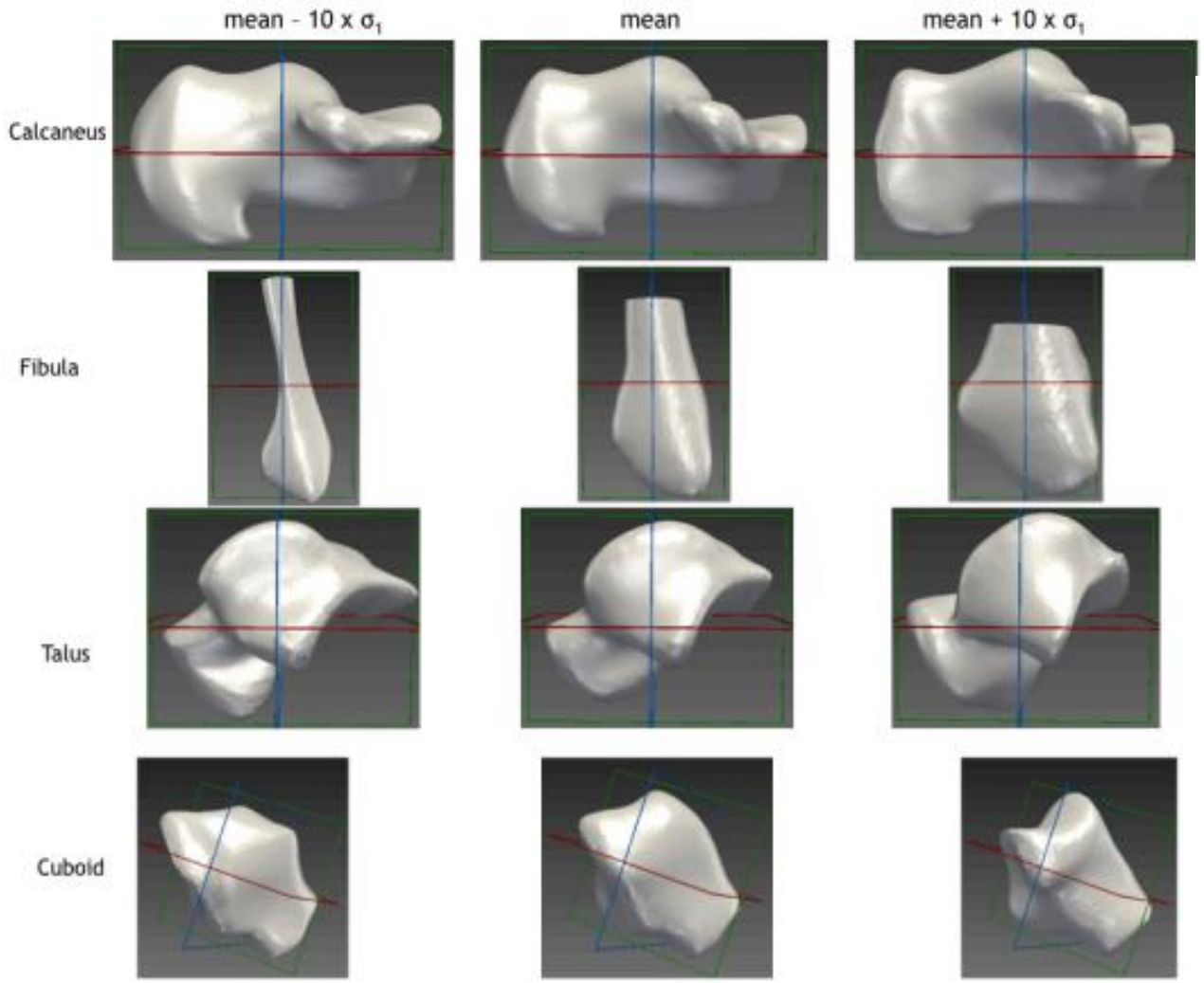

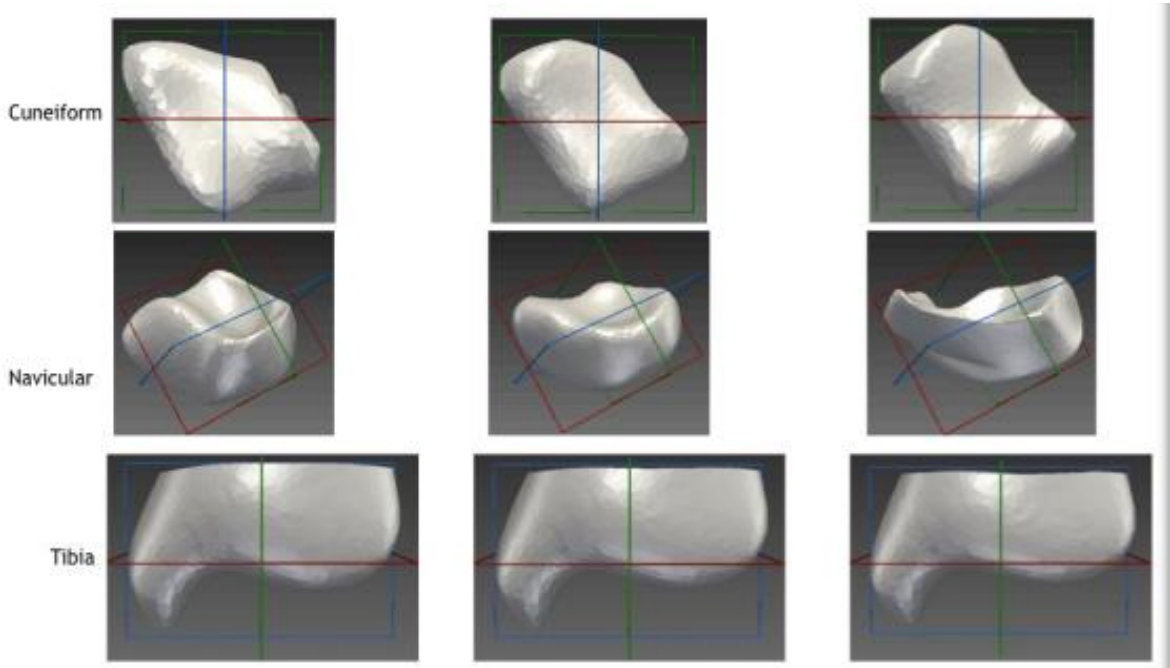

Applying ASM to automatic segmentation

- Gradient of image to identify edges, initialize mean model to them
- Iteratively update shape vector b and deform vertices of model
- Continue until best fit to gradient edges

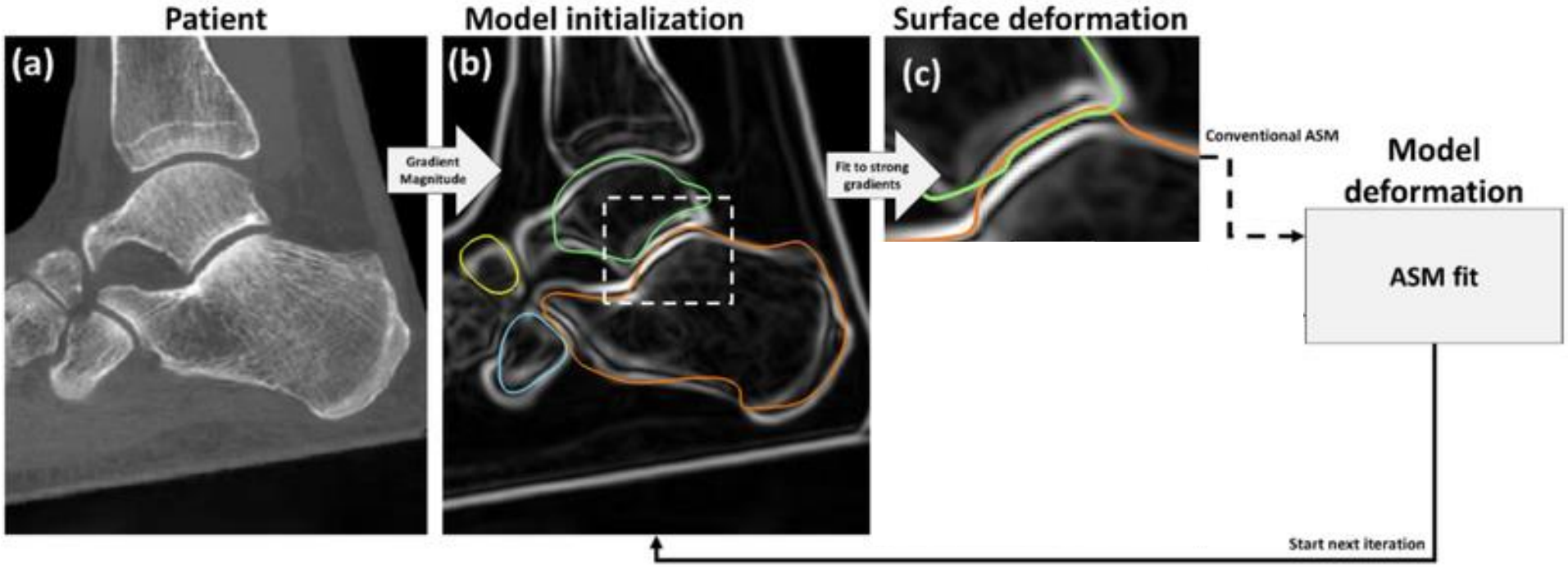

Calculating Segmentation Error

- Surface Error is sum of squared distances between edge vertices of test segmentation and manual ground truth segmentation
- Root mean square distance is RMS of surface error for all points

$$\text{surf\_err}_i = \sqrt{(x_i - x_{nn,i})^2 + (y_i - y_{nn,i})^2 + (z_i - z_{nn,i})^2}$$

$$\text{RMSD} = \sqrt{\left[\sum_1^N (surf\_err_i\ )^2\right] / N}$$

Paper 1: Methodology

- Use ASM to segment ankle bones and map articular surfaces
- Detect implants as cylindrical approximations

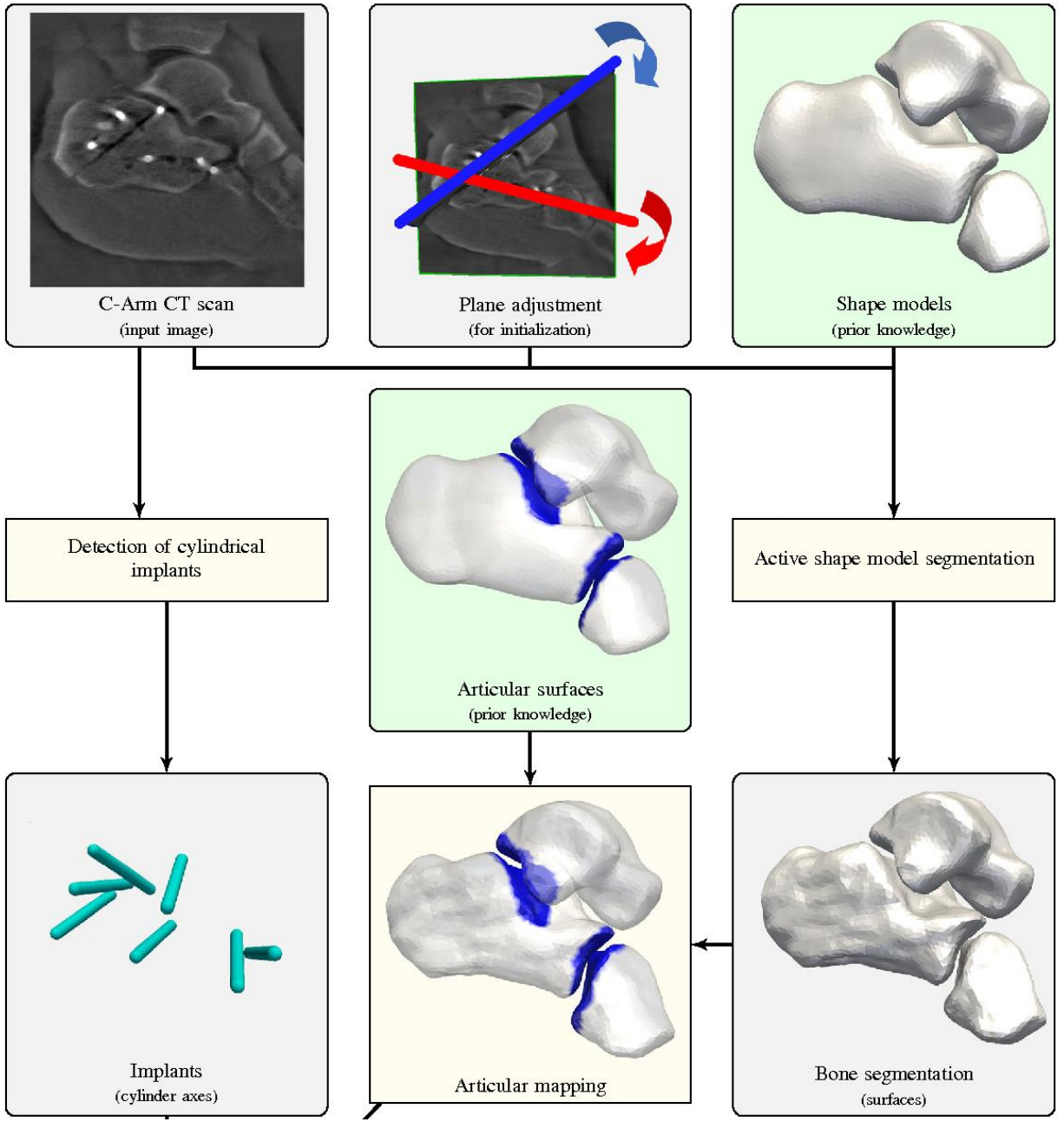

Paper 1: Cadaver Study

- Implants are inserted into cadaver ankles
- Locations of implant articular intersection are manually annotated in image as ground truth
- Locations are also automatically detected and error calculated

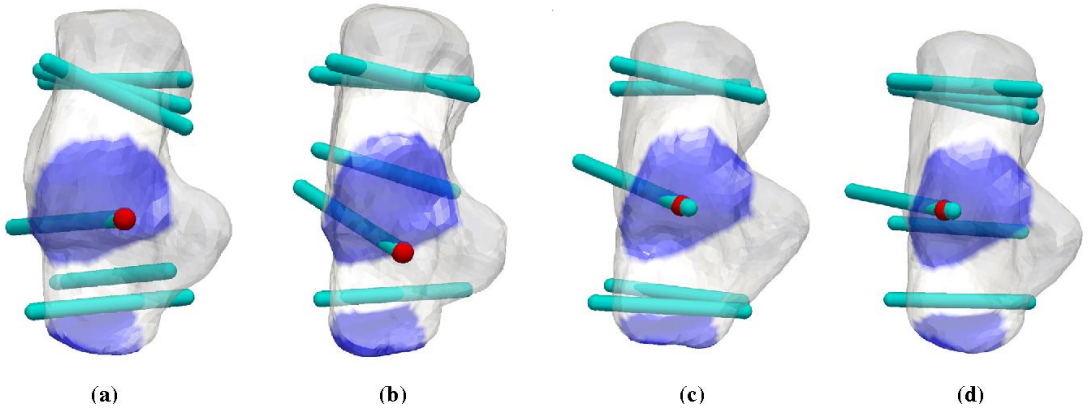

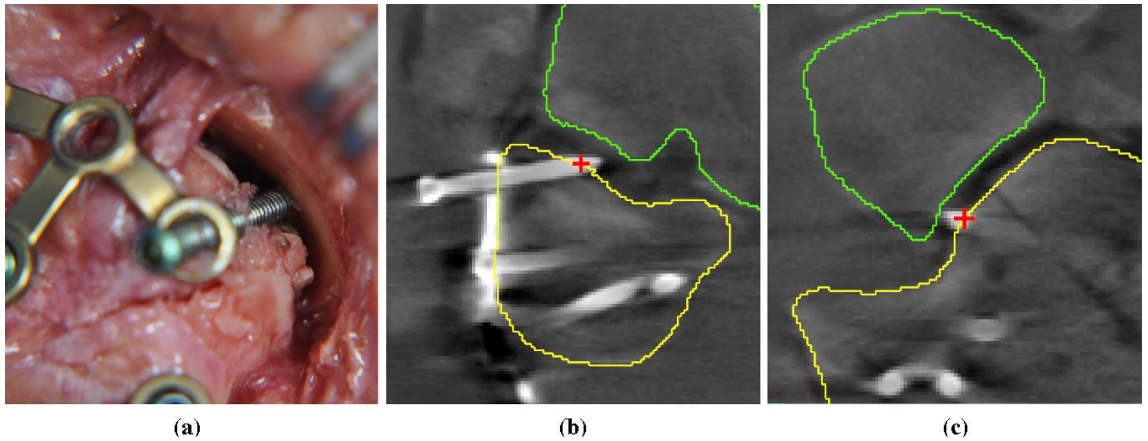

Paper 1: Results and Significance

- Average surface segmentation errors of 0.81 , 0.45 and 0.59 mm for calcaneus, talus, and cuboid respectively
- Able to compensate suboptimal initializations to certain extent
- Cadaver test: position of implants localized with 0.80 mm error on average
- Shows reliable segmentation in retrospective patient data, ability to localize implants accurately

Method bone	ASD bone (mm)	ASD LA (mm)	ASD CC (mm)
Multiple ASMs with optimal surface integration			
"Active shape models" section			
Calcaneus	0.81 ± 0.13	0.76 ± 0.29	0.66 ± 0.24
Talus	0.45 ± 0.18	0.44 ± 0.09	
Cuboid	0.59 ± 0.27		0.38 ± 0.10
Model-independent regions			
"Model-independent regions" section			
Calcaneus	0.79 ± 0.14	0.59 ± 0.29	0.46 ± 0.16
Talus			
Cuboid			$) \pm 0.09$
Deforma			
Heimann			
Calcan			4 ± 0.24
Talus			
Cuboid			1 ± 0.12

The erro
ankle joi

the lower

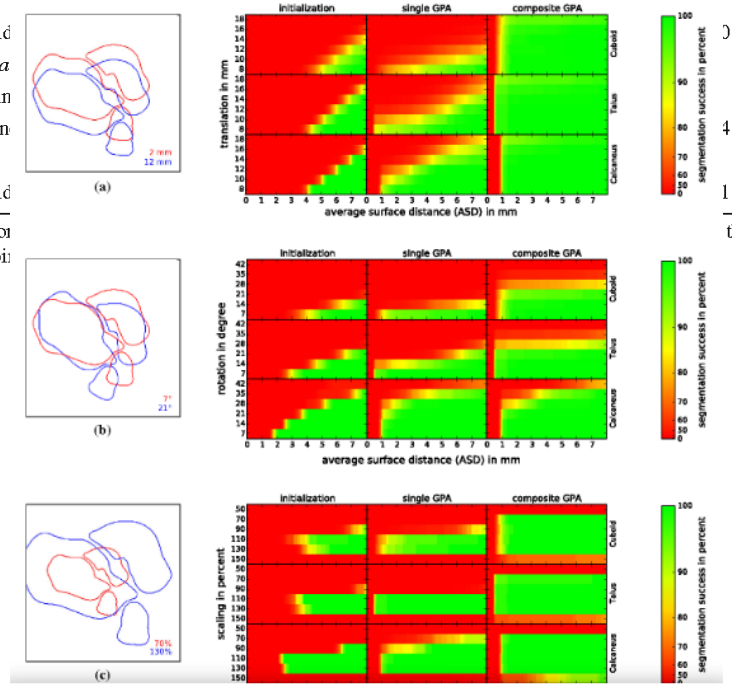

Paper 1: Assessment

Pros

- Validated theoretical ASM framework for automatic ankle segmentation
- High segmentation accuracy (sub-mm RMSD)
- Clinical relevance shown through cadaver study

Cons

- Only focused on 3 bones while there are 7 total in ankle joint
- Vulnerable to poor initializations
- Improvement over manual/standard of care for implant localization not necessarily shown by cadaver study

Paper 2: Purpose and Significance

- Improve traditional ASMs in narrow joint spaces (prevent overlaps)
- Improve poor initialization due to unreliable gradients (low contrast, noise)
- All 7 ankle bones

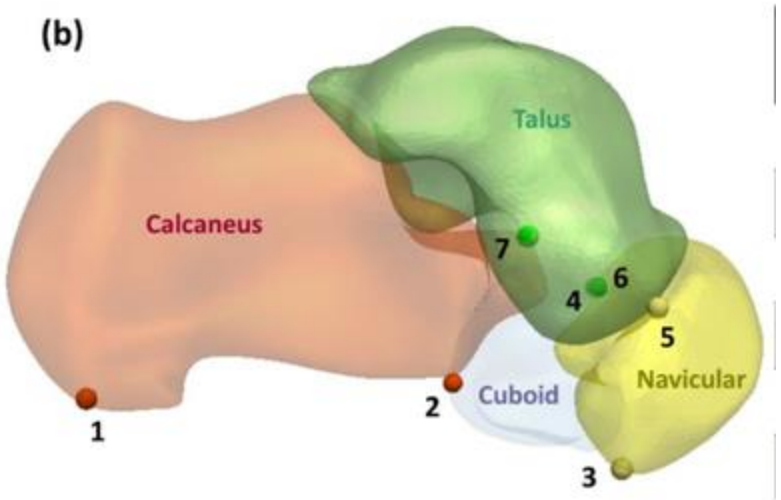

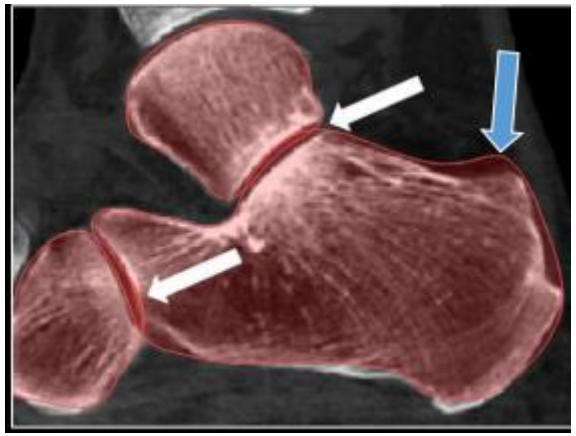

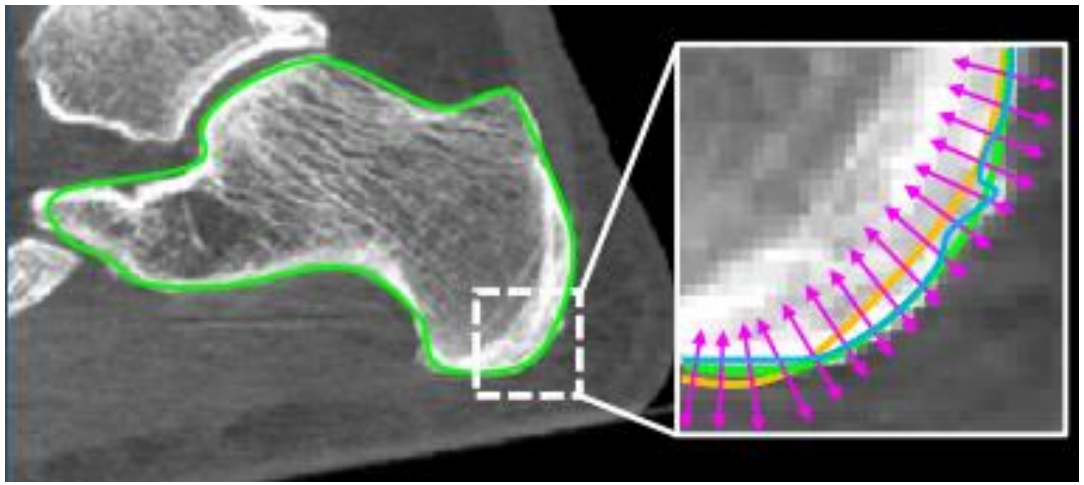

Articular Surface Distances	Min [mm]	Max [mm]	Mean [mm]
Calcaneus to Cuboid	0.35	1.66	1.46
Calcaneus to Talus	0.55	11.58	5.49
Cuboid to Calcaneus	0.52	4.62	2.17
Cuneiform to Navicular	1.78	3.60	2.87
Fibula to Talus	1.41	7.40	3.41
Fibula to Tibia	3.17	8.25	4.91
Navicular to Cuneiform	0.64	2.04	1.62
Navicular to Talus	1.14	4.55	2.21
Talus to Calcaneus	0.50	12.68	5.68
Talus to Fibula	1.41	5.34	3.01
Talus to Navicular	0.31	3.90	1.51
Talus to Tibia	1.24	5.43	2.31
Tibia to Fibula	3.17	8.35	5.14
Tibia to Talus	1.24	7.03	2.57

Paper 2: Coupled Active Shape Models (cASMs)

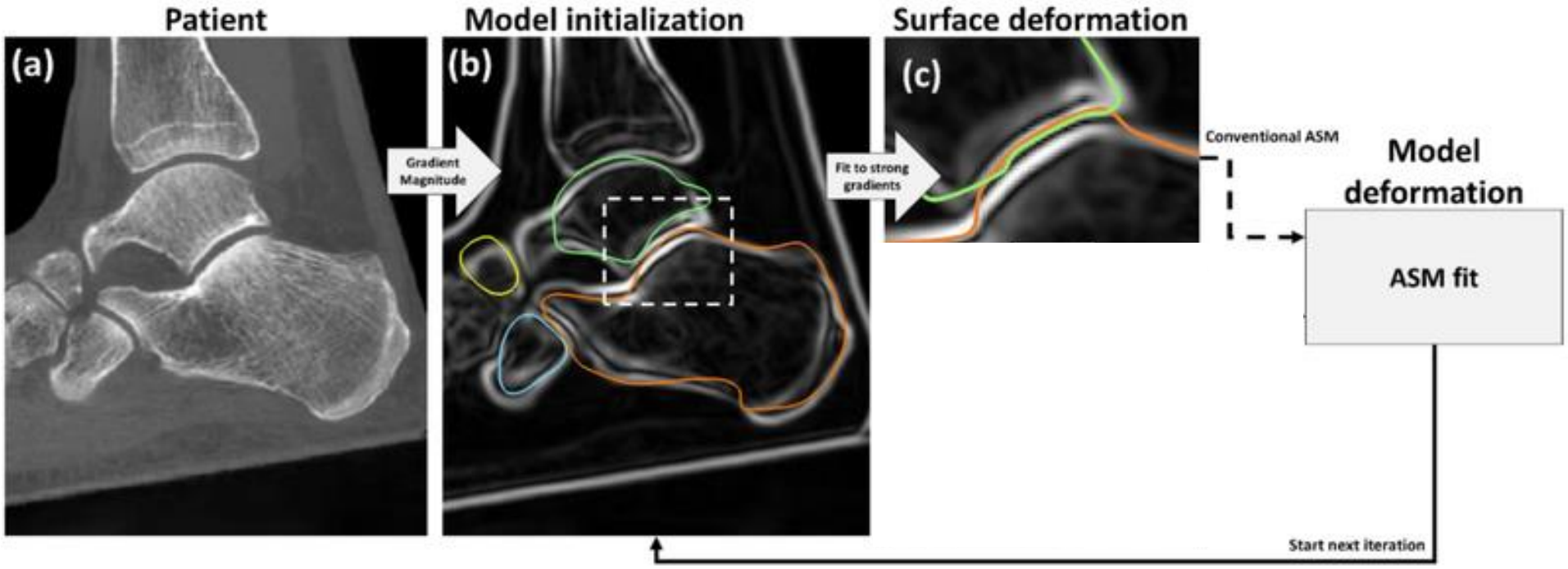

Paper 2: Coupled Active Shape Models (cASMs)

- Simultaneously fit multiple bones to take into account distance between them

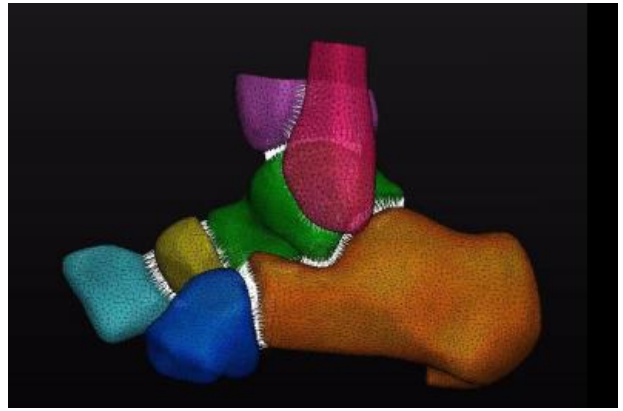

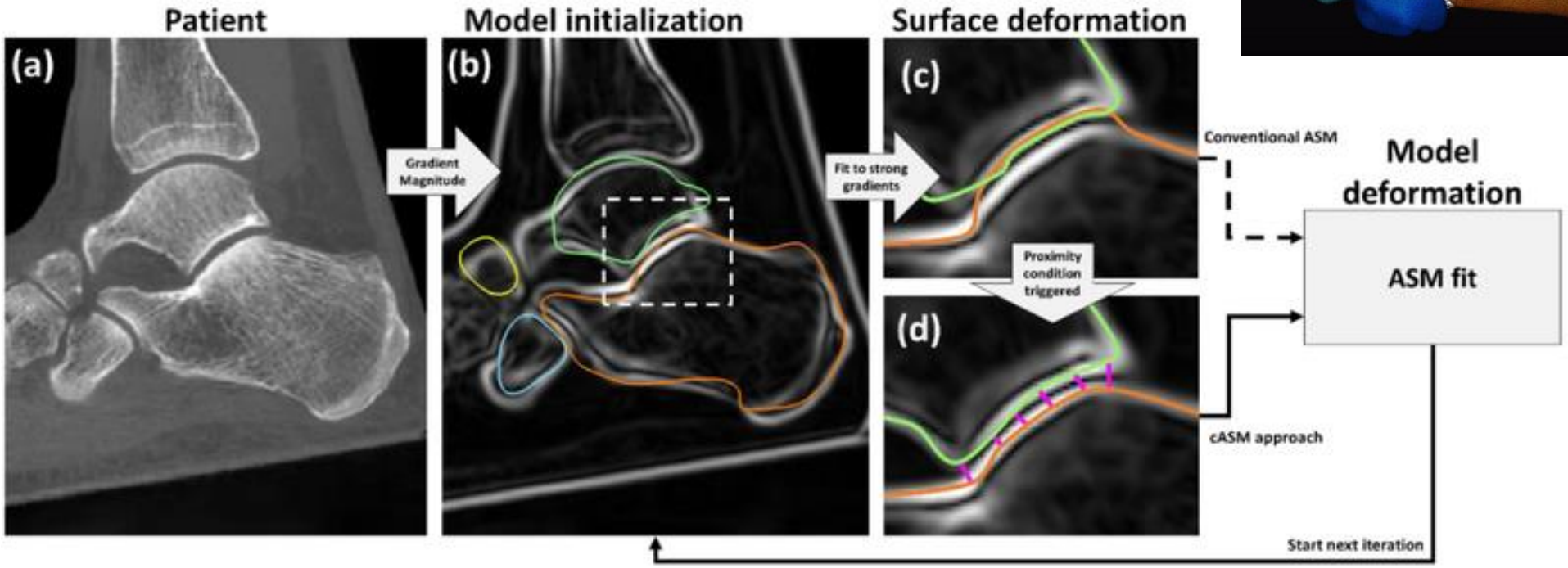

Paper 2: Results and Significance

- Test set of 21 (Leave-one-out)
- Never allows overlap
- Improved segmentation when gradients are weak
- Collisions were detected and corrected in 50-80% of test cases depending on bone

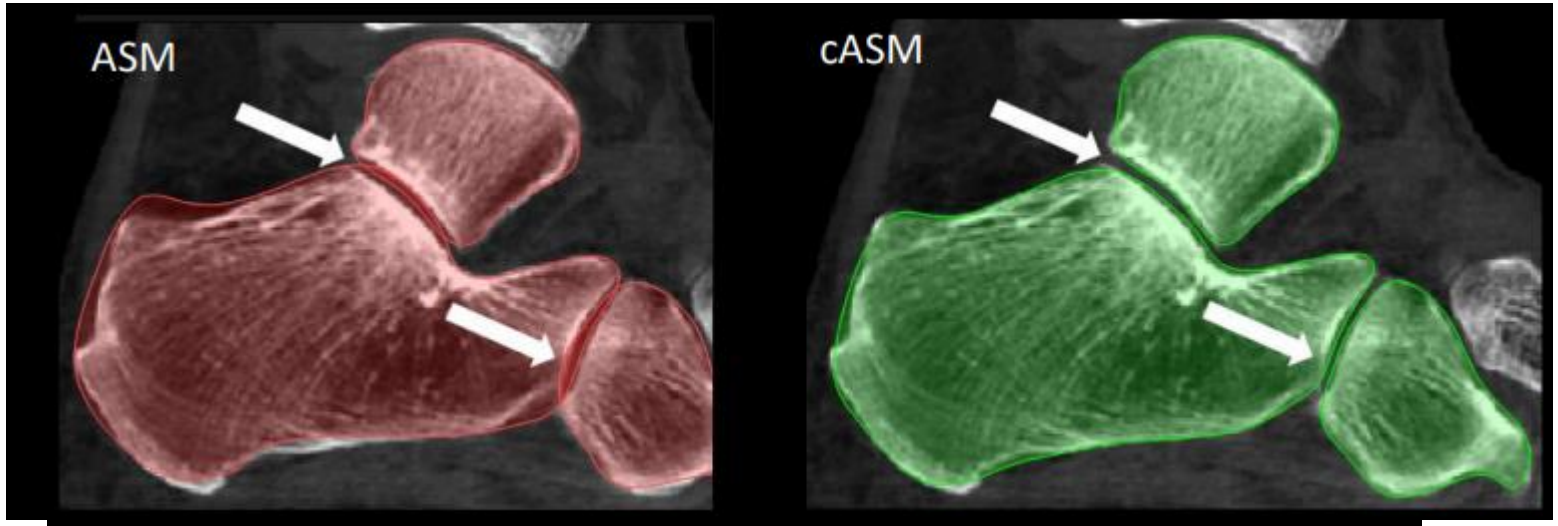

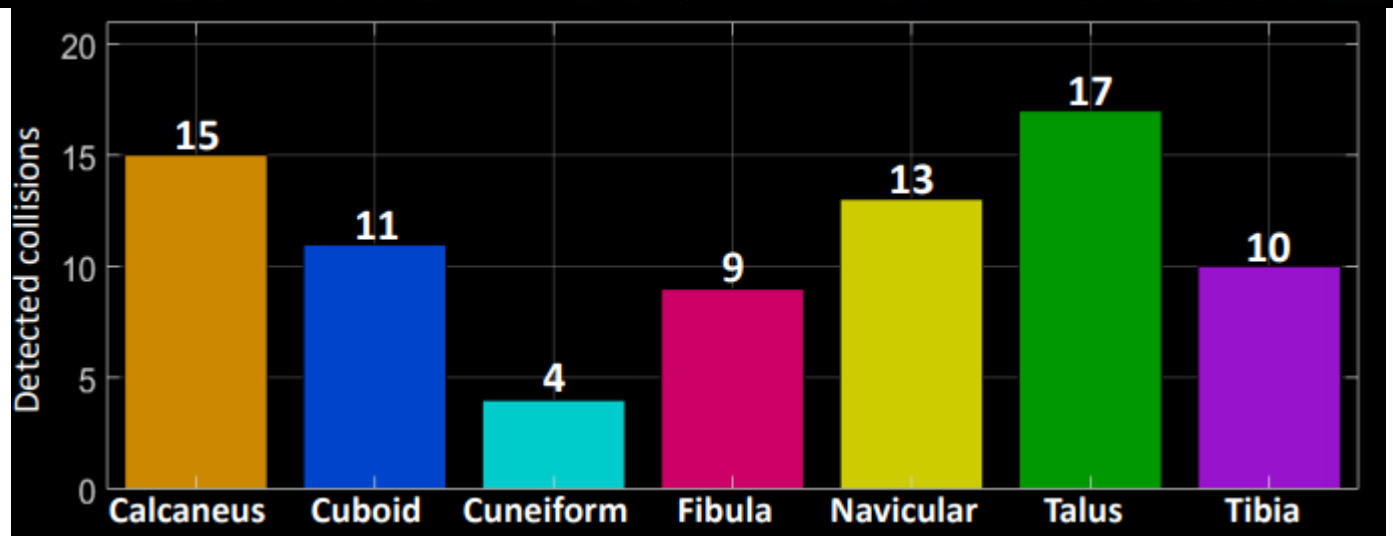

Paper 2: Results and Significance

- Improved Segmentation Accuracy Overall (RMSD of 2.7 mm of cASM vs. 3.6 mm with ASM)
- Faster convergence (~40 vs ~60 iterations)
- 25-55% error reduction in landmark positions

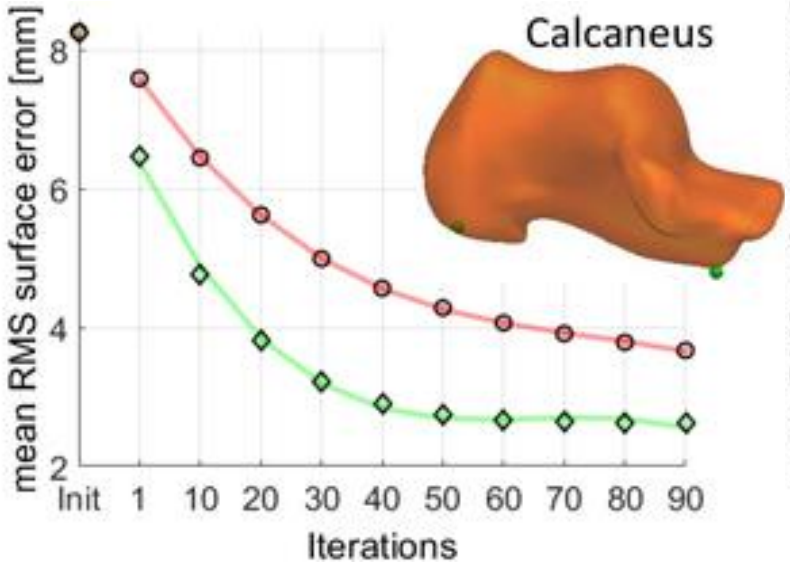

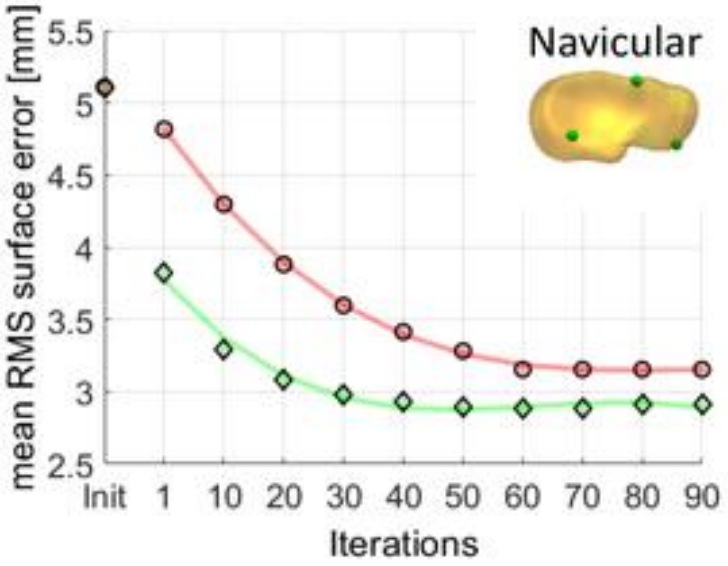

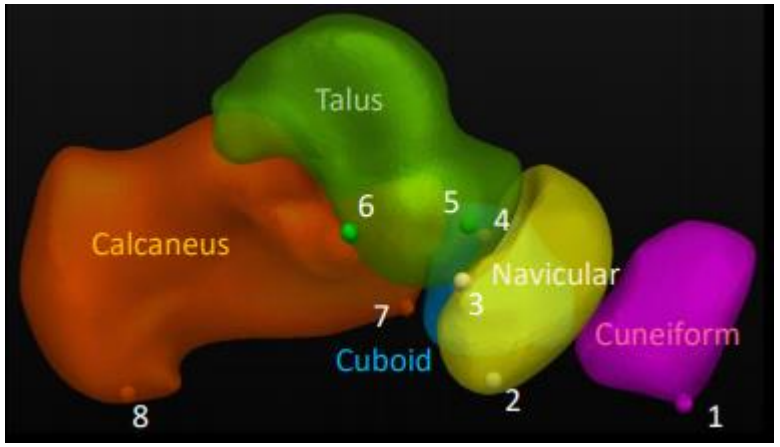

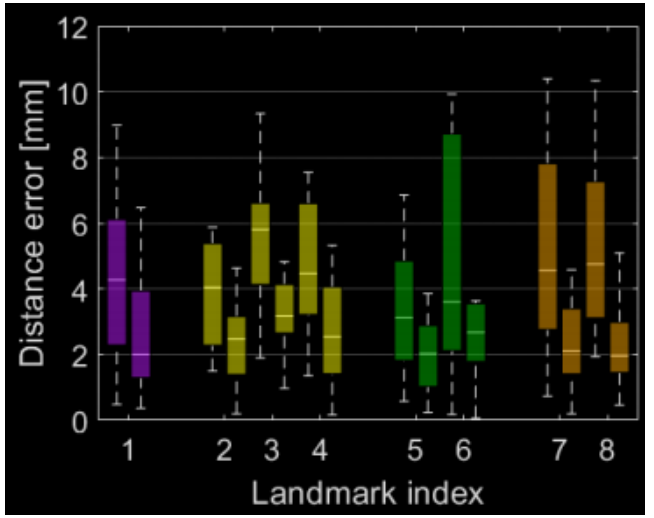

Paper 2: Assessment

Pros

- Demonstrated improved accuracy of segmentations with cASM over ASM, especially in narrow spaces between bones
- Also showed detection and correction of collisions, faster convergence, and improved landmark accuracy
- Many potential envisioned clinical applications

Cons

- Somewhat small sample size of 21, increasing this may help with further reduction of error
- May still be prone to artifacts like metal or surgical tools or poor image quality
- Clinical applications and relevance yet to be proven